MNRAS 000, 1–5 (2020) Preprint 1 March 2022 Compiled using MNRAS LATEX style file v3.0

Revised instellation patterns for close-in exoplanets

Mradumay Sadh ★

Accepted 2020 September 15. Received 2020 September 7; in original form 2020 July 31

ABSTRACT

The distribution of instellation at the top of a planet's atmosphere or surface is usually calculated using the inverse-square law of radiation. This is based on the assumption that the host star is far enough to be considered a point-sized Lambertian source. This assumption, which works well for the solar system planets and most exoplanets, must be revised for close-in exoplanets. The objective of this work is to derive accurate instellation patterns for close-in exoplanets, for which the effects of the spherical shape of the star must be taken into account. First an analytical formula of the insolation as a function of latitude was derived, taking the star and the planet as 3-D bodies, and incorporating the limb darkening effects of the star. Then numerical techniques were used to compute the distribution of the insolation on close-in planets as a function of latitude for a wide range of stellar and planetary properties.There are significant deviations in instellation values and their distribution on close-in exoplanets, due in similar proportions to the physical size of the star and stellar limb-darkening effects. The insolation at the susbtellar point is always higher – by as much as 21% for known exoplanets – than the standard calculation. The substellar longitude of the terminator can significantly extend on the nightside, from 90° up to 110° for known exoplanets.

Key words: Radiative Transfer– Stars:fundamental parameters – Planets and satellites:fundamental parameters

1 INTRODUCTION

Instellation is one of the major factors that govern the climate of an exoplanet. Precise instellation values and their distribution above the atmosphere is therefore essential for climate modelling. The inverse-square (IS) law of instellation suffices for a vast majority of the extra-solar planet population. It turns out that the IS law is based on a few facile assumptions. This approach attempts to reform these assumptions. To understand these, let's assume the star as a point-sized object at the origin of our coordinate system demonstrated as a bright yellow spot in Fig. 1. The distance of the star to the substellar point in this assumption is elementary and given by $a - R_p$ where a is the semi-major axis that is, $(R_p + R_\star + d)$ viz., the sum of planetary-and-stellar radius and the distance between the surfaces. We can then write the IS law as:

$$I = \frac{L_b cos\theta_{\rm p}}{4\pi(a - R_p)^2} \tag{1}$$

where L_b is the bolometric luminosity. This equation has been used for previous studies of close-in exoplanets to construct atmospheric thermal structures (Stevenson et al. 2014). Since the star has a physical size, we see that the distance of the substellar point from the surface of the star is not a constant but instead variable at every point on the star. Additionally, due to large distance, the incident radiation in IS law is assumed to have a planar wave-front. Due to this, the angle subtended by the radiation is dependent on only one variable that is, the latitude ($\theta_{\rm p}$). Also, the IS law doesn't account for the limb darkening effects of the star. For exoplanets with semi-major axes less than ten times their host-star radius, these assumptions break down.

When we derive an equation taking close-in exoplanets into account, it is imperative to reform these assumptions. The paper is structured as follows. In section 2, an equation is derived for instellation using a 3-D geometrical formulation and limb darkening effects for a surface element on the star and then integrated for the whole star. The integration of this equation by analytic means happens to be complicated and cumbersome. Therefore, numerical integration methods are used to solve this integral. The results section depicts the effects of this model for a few close-in exoplanets. Subsequently, an analysis about the cases where this model significantly differs from the IS law and the reason behind these differences is presented. Lastly, there is a discussion about the applicability of the model, observational tests, and further scope for improvement.

2 METHODS

The IS law is well defined for a point-sized source. A spherical body can be assumed to be made up of many such point-size sources. To calculate the net irradiance or instellation due to a spherical source(star) on a planet, we need to integrate the radiation emanating from all points on this star. Previous studies by Wilson (1990), Budaj (2011), Chen & Rhein (1969), and Horvat et al. (2019) have used a fairly similar approach to calculate the bolometric radiance for modeling the light curves of close binary stars. They also incorporate the reflection of radiation between the binary components to estimate the radiosity. This model doesn't include the reflection effects and doesn't calculate the radiosity and radiance. Instead, this model calculates the irradiance due to the star on the planet. Only bolometric quantities are used in this derivation. Also, this model uses the non-linear limb darkening law as opposed to the linear and quadratic laws used in previous models. The work by Wood (1973)

★ E-mail: mradumay137@gmail.com

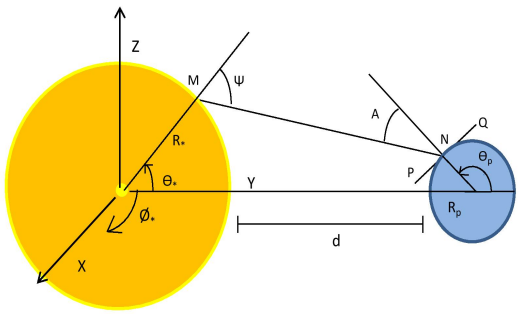

Figure 1. Spherical geometry of the star($R_\star$) and planet(R_p) depicting the incident ray(MN),local horizon(PQ) and normal lines to the stellar and planetary surface under consideration.

is useful to understand the essence of this model. Wood (1973) uses a similar approach. However, in his analysis, he aims to establish an analytical relation without integration by using quasi-empirical methods. This model attempts to include all the intricacies of the problem and take advantage of the advanced computational power of numerical methods of integration to derive the results. To get the net instellation we need to integrate all irradiance values for the stellar surface visible to the planet. Assuming the star and planet to be spherical, we choose an arbitrary point on the star and calculate the irradiance on an arbitrary point on the planet as illustrated in Fig. 1.

2.1 Description of the star-planet system in 3-D geometry

We can express any point in Cartesian coordinates on the stellar sphere as:

$$x_\star = R_\star cos\theta_\star sin\phi_\star$$

$$y_\star = R_\star cos\theta_\star cos\phi_\star$$

$$z_\star = R_\star sin\theta_\star$$

where $\theta_\star$ and $\phi_\star$ define the latitude and longitude of the host star, respectively. The angle θ is measured along the YZ plane and ϕ along the XY plane. Likewise, we can express any point in Cartesian coordinates on the planetary sphere as:

$$x_\mathrm{p} = R_p cos\theta_\mathrm{p} sin\phi_\mathrm{p}$$

$$y_\mathrm{p} = R_p + R_\star + d + R_p cos\theta_\mathrm{p} cos\phi_\mathrm{p} = a + R_p cos\theta_\mathrm{p} cos\phi_\mathrm{p}$$

$$z_\mathrm{p} = R_p sin\theta_\mathrm{p}$$

where θ_p and ϕ_p define the latitude and longitude of the planet, respectively. Here, d is the shortest distance between the surfaces of the planet and the star and $(R_p + R_\star + d)$ is the semi-major axis(a). The star is assumed to have a total bolometric luminosity L_b and effective temperature $T_\star$. For a surface element dS on the star, the power dL_b emitted by this surface is given by the Stephan-Boltzmann law as:

$$dL_b = \sigma {T_\star}^4 dS = \frac{L_b {R_\star}^2 cos\theta_\star d\theta_\star d\phi_\star}{4\pi {R_\star}^2} = \frac{L_b cos\theta_\star d\theta_\star d\phi_\star}{4\pi}$$

The standard equation for irradiance or the power per unit area incident on a surface with an arbitrary area vector, for a source with power dL, is expressed as: (McCluney 2014)

$$\int dI = \oiint_S \frac{dL_b cosA}{2\pi (d_s)^2} \tag{2}$$

To make the calculations easy, we can calculate these instellation values along the substellar longitude on the planet since the planet can be considered a 2-D body in this case. Now we evaluate the general expressions for distance(d_s) and angle A.

2.2 Calculation of the distance between the stellar and planetary spheres

For this calculation we need to evaluate the Euclidean distance between any set of arbitrary points on the star and the planet or, in other words, the length of the line segment MN in Fig.1. Using the Cartesian coordinates introduced before, we have:

$$d_s = \Big[(R_\star sin\theta_\star - R_p sin\theta_\mathrm{p})^2 + (R_\star cos\theta_\star sin\phi_\star - R_p cos\theta_\mathrm{p} sin\phi_\mathrm{p})^2 + (R_\star cos\theta_\star cos\phi_\star - R_p - R_\star - d - R_p cos\theta_\mathrm{p} cos\phi_\mathrm{p})^2 \Big]^{1/2}$$

2.3 Angle between area vector and incident ray from the surface element

The angle between the incident ray from the star(MN) and the area vector of the receiving surface is given by A as shown in Fig.1. If the direction cosines of MN and the area vector are l_1, l_2, l_3 and m_1, m_2, m_3 respectively, then the angle between them is derived by taking a dot product of two unit vectors along these lines:

$$cosA = l_1 m_1 + l_2 m_2 + l_3 m_3 \tag{3}$$

The direction cosine of the area vector is given by:

$$m_1 = \frac{x_p}{R_p} = cos\theta_\mathrm{p} sin\phi_\mathrm{p}$$

$$m_2 = \frac{y_p}{R_p} = cos\theta_\mathrm{p} cos\phi_\mathrm{p}$$

$$m_3 = \frac{z_p}{R_p} = sin\theta_\mathrm{p}$$

Similarly, the direction cosine of the incident ray is given by:

$$l_1 = \frac{x_p - x_\star}{d_s} = \frac{R_p cos\theta_\mathrm{p} sin\phi_\mathrm{p} - R_\star cos\theta_\star sin\phi_\star}{d_s}$$

$$l_2 = \frac{y_p - y_\star}{d_s} = \frac{R_p + R_\star + d + R_p cos\theta_\mathrm{p} cos\phi_\mathrm{p} - R_\star cos\theta_\star cos\phi_\star}{d_s}$$

$$l_3 = \frac{z_p - z_\star}{d_s} = \frac{R_p sin\theta_\mathrm{p} - R_\star sin\theta_\star}{d_s}$$

Using equation 3 and substituting the values of the direction cosines, we get:

$$cosA = \frac{R_\star [-cos\theta_\star cos\theta_\mathrm{p} \cos(\phi_\star - \phi_\mathrm{p}) - sin\theta_\star sin\theta_\mathrm{p}]}{d_s} + \frac{(R_p + R_\star + d) cos\theta_\mathrm{p} cos\phi_\mathrm{p} + R_p}{d_s}$$

It is crucial to incorporate the essential geometrical factors which affect the limits of the integral in equation 2. These are discussed in the following subsection.

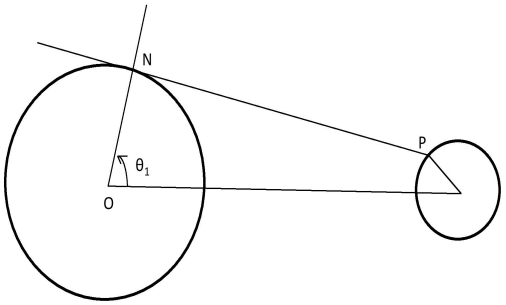

Figure 2. Tangent to the stellar surface(NP) determines the integral limit

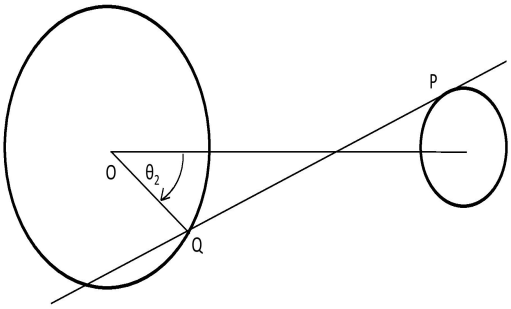

Figure 3. The point of intersection of the local horizon PQ with the stellar circle constraints the lower limit of the integral

2.4 Geometrical Factors

2.4.1 Apparent surface

The apparent surface of the host star visible to a close-in planet depends on the star-planet distance. If the planet is far enough from the star, one can see the entire hemisphere of the star. However, as we approach closer, we only see a region bound between the tangents to the stellar circle from the point of observation on the planet. Fig. 2 demonstrates that a tangent from a point P on the planet determines the limit of what is visible to the observer. The angle θ_1 hence determines the limit of integration. The procedure to calculate θ_1 is as follows.
Using the coordinates introduced in the previous subsection, we substitute $\phi = 0$ since the calculation is limited to the YZ plane. The slope of the tangent NP is given by:

$$m_1 = \frac{z_\star - z_p}{y_\star - y_p}$$

Therefore,

$$m_1 = \frac{R_\star sin\theta_\star - R_p sin\theta_\mathrm{p}}{R_\star cos\theta_\star - (a + R_p cos\theta_\mathrm{p})}$$

Since the tangent and normal to the stellar circle are perpendicular to each other, the slope of the normal to the stellar circle(ON) can be calculated using the general relation between the slopes of two mutually perpendicular lines with slopes m_1 and m_2, that is :

$$m_1 m_2 = -1$$

Therefore, slope of ON is given by,

$$m_2 = tan\theta_\star = \frac{a + R_p cos\theta_\mathrm{p} - R_\star cos\theta_\star}{R_\star sin\theta_\star - R_p sin\theta_\mathrm{p}} \tag{4}$$

To simplify equation 4, we first divide both numerator and denominator by $cos\theta_\star$:

$$tan\theta_\star = \frac{(a + R_p cos\theta_\mathrm{p}) sec\theta_\star - R_\star}{R_\star tan\theta_\star - R_p sin\theta_\mathrm{p} sec\theta_\star}$$

After rearranging terms we have:

$$R_\star tan^2\theta_\star - R_p sin\theta_\mathrm{p} sec\theta_\star tan\theta_\star = (a + R_p cos\theta_\mathrm{p}) sec\theta_\star - R_\star$$

$$R_\star sec\theta_\star = R_p sin\theta_\mathrm{p} tan\theta_\star + a + R_p cos\theta_\mathrm{p}$$

Now we square this expression and define $\beta = a + R_p cos\theta_\mathrm{p}$
Consequently, we get:

$$sec^2\theta_\star(R_\star^2 - R_p^2 sin^2\theta_\mathrm{p}) - 2\beta R_\star sec\theta_\star + \beta^2 + R_p^2 sin^2\theta_\mathrm{p} = 0$$

Solving this quadratic equation and assuming $\beta \sim a$ we get:

$$\cos\theta_\star = \cos\theta_1 = \frac{R_\star + R_p sin\theta_\mathrm{p}}{a} \tag{5}$$

It should be noted that equation 5 accommodates all possible cases of the star-planet system, including hypothetical cases that are less likely to be found observationally. For all practical purposes, we can ignore the radius of the planet in equation 5 without appreciably changing the results. We can now calculate θ_1 at any given value of θ_p and can express the formula for instellation as:

$$I = \int_{-\theta_1}^{\theta_1}\int_{-\theta_1}^{\theta_1} \frac{L_b cos\theta_\star d\theta_\star d\phi_\star}{8\pi^2} \frac{cosA}{d_s^2} \tag{6}$$

2.4.2 Stellar surface above local horizon

For higher latitudes on close-in exoplanets, a part of the stellar surface is hidden beneath the local horizon. This is taken into account by integrating the surface above the local horizon. In Fig. 3, we can see that the stellar surface below Q lies beneath the local horizon PQ and is hence neglected. Since an incident ray grazing through the local horizon would be perpendicular to the normal vector through that point on the planet, therefore, to obtain the corresponding angle(θ_2) determined by the point of intersection of the local horizon with the stellar circle, we put cosA=0 in equation 3. Again, we neglect $\phi_\star$ and only consider the polar angle($\theta_\star$). When we solve specifically for $\theta_\star$, we get a quadratic equation with the following roots:

$$\cos\theta_2 = \frac{cos\theta_\mathrm{p}((R_p + R_\star + d)cos\theta_\mathrm{p} - R_p)}{R_\star} \pm \frac{sin\theta_\mathrm{p}(R_\star{}^2 - ((R_p + R_\star + d)cos\theta_\mathrm{p} - R_p)^2)^{1/2}}{R_\star}$$

θ_2 obtained from the above equation determines the limit of integration for higher latitudes. Therefore, equation 6 now becomes:

$$I = \int_{-\theta_2}^{\theta_1}\int_{-\theta_1}^{\theta_1} \frac{L cos\theta_\star d\theta_\star d\phi_\star}{8\pi^2} \frac{cosA}{d_s^2} \tag{7}$$

For brevity, we use $\forall$ symbol to imply for all.
$\forall\ \pi - \theta_\mathrm{p} > 0$, θ_2 is given by:

$$\cos\theta_2 = \frac{cos\theta_\mathrm{p}((R_p + R_\star + d)cos\theta_\mathrm{p} - R_p)}{R_\star} + \frac{sin\theta_\mathrm{p}(R_\star{}^2 - ((R_p + R_\star + d)cos\theta_\mathrm{p} - R_p)^2)^{1/2}}{R_\star}$$

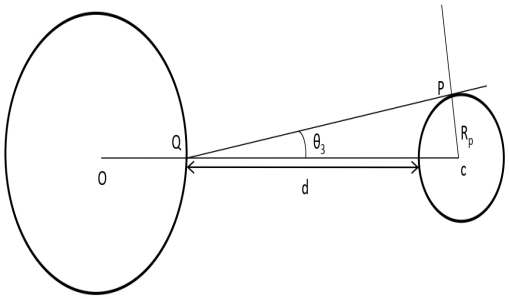

Figure 4. Lower limit of the integral becomes positive after a certain latitude on the planet determined by $\pi/2 - \theta_3$

and $\forall\ \pi - \theta_p < 0$ we have:

$$\cos\theta_2 = \frac{cos\theta_p((R_p + R_\star + d)cos\theta_p - R_p)}{R_\star} - \frac{sin\theta_p({R_\star}^2 - ((R_p + R_\star + d)cos\theta_p - R_p)^2)^{1/2}}{R_\star}$$

The equation 6 in this case would be:

$$I = \int_{-\theta_1}^{\theta_2}\int_{-\theta_1}^{\theta_1} \frac{Lcos\theta_\star d\theta_\star d\phi_\star}{8\pi^2}\frac{cosA}{d_s^2}$$

$\forall\ \pi - \theta_p > \theta_1$, one of the polar angle limits will be modified to θ_2. In addition to this, another intricacy needs to be addressed. After a certain latitude, the lower limit of the integral will be positive since the local horizon will intersect the star above its equatorial plane. The latitude at which the lower limit is zero is given by $\pi/2 - \theta_3$, as shown in Fig. 4.
Therefore, $\forall\ \pi - \theta_p > \pi/2 - \theta_3$, equation 7 becomes:

$$I = \int_{\theta_2}^{\theta_1}\int_{-\theta_1}^{\theta_1} \frac{Lcos\theta_\star d\theta_\star d\phi_\star}{8\pi^2}\frac{cosA}{d_s^2}$$

The angle θ_3 can be calculated using basic trigonometry as,

$$\sin\theta_3 = \frac{R_p}{R_p + d} \tag{8}$$

However, this factor only comes into play when the planet is much closer to its host star. In fact, so close that the distance between the stellar and planetary surface is comparable to the planetary radius.

2.4.3 Limb Darkening

Hitherto it has been assumed that the star is a perfect black-body. However, the stellar photosphere is prone to absorption and scattering of the emitted light that adds a level of intricacy to the former assumption. A star appears to be more bright around the centre and less bright near the limbs. In other words, there exists a temperature gradient across the stellar photosphere. As a result, each surface element on the star has a different temperature. Therefore, it becomes imperative to include the effect of this gradient.

We can use the non-linear limb darkening model proposed by Claret (2000) due to its accuracy and applicability to the whole HR diagram. The equation for limb darkening in the Claret (2000) model is given by:

$$I(\mu) = I(0)[1 - a_1(1-\mu)^{1/2} - a_2(1-\mu) - a_3(1-\mu)^{3/2} - a_4(1-\mu)^2] \tag{9}$$

Further we can define,

$$F(\psi) = 1 - a_1(1-\mu)^{1/2} - a_2(1-\mu) - a_3(1-\mu)^{3/2} - a_4(1-\mu)^2 \tag{10}$$

Here I is the bolometric intensity, a_1, a_2, a_3, a_4 are bolometric limb darkening coefficients, and μ is given by,

$$\mu = cos\psi$$

Where, ψ is the angle between the line of sight and the normal to the surface of the star, as shown in Fig. 1. This angle can be calculated using equation 3 by replacing the normal to the planetary surface by normal to the stellar surface. For all practical purposes, we can ignore the radius of the planet to make the calculation easy.

$$cos\psi = \frac{R_\star - (R_\star + d)cos\theta_\star cos\phi_\star}{d_s} \tag{11}$$

2.5 Final equation for instellation distribution

If we include the stellar limb darkening effects and other geometrical effects, then the equation culminates to:

$$I = \int_{-\theta_1}^{\theta_1}\int_{-\theta_1}^{\theta_1} \frac{L(\psi)cos\theta_\star d\theta_\star d\phi_\star}{8\pi^2}\frac{cosA}{d_s^2} \tag{12}$$

Now, the luminosity is a function of ψ. The luminosity of a surface element on the star depends on the optical depth at that surface and hence the temperature of the surface.

$$L(\psi) = \sigma T^4(\psi) 4\pi {R_\star}^2 = \sigma T_0^4 F(\psi) 4\pi {R_\star}^2$$

If we substitute the value of $F(\psi)$ from equation 10, we get the final expression that we integrate with conditional limits discussed in the previous subsections.

$$I = \int_{-\theta_1}^{\theta_1}\int_{-\theta_1}^{\theta_1} \frac{\sigma T_0^4 F(\psi){R_\star}^2 cos\theta_\star d\theta_\star d\phi_\star cosA}{2\pi(d_s)^2} \tag{13}$$

Here, T_o is the temperature at an optical depth of 1.

The analytical solution for this integral is intricate to obtain due to the complex nature of the limits. It is possible to use standard solutions of elliptic integrals to solve the integral analytically. However, it cannot be done without introducing over-simplistic assumptions, and it is cumbersome to solve. Therefore,numerical methods have been used to solve the integral.
The limb darkening coefficients are calculated according to a given temperature, surface gravity and metallicity using the Claret (2000) data. The limb darkening coefficients in this data are computed using the PHOENIX model for stellar temperatures from 2000 to 9800 K, log of surface gravity ranging from 3.5 to 5, and assuming solar metallicity. A multi-linear interpolation is then performed on this data to obtain the required coefficients according to the given stellar parameters.

3 RESULTS AND DISCUSSION

For Earth, the results are in accordance with the IS law as shown in Fig. 5. The solar constant is obtained as 1354.04 W/m^2 which is well in agreement with the experimental solar constant measurements Fröhlich (2000). Instellation patterns are presented for close-in planets Kepler-10 b, 55 Cancri e, CoRoT-7 b and K2-137 b in Fig. 6.

An important distinction between the two approaches comes at the poles of the exoplanet. The IS law predicts zero instellation since it follows a cosine relation of instellation with latitude. Therefore, for a latitude of 90 degrees, the instellation becomes zero. This model

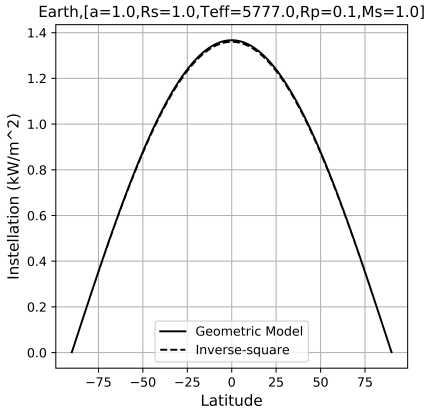

Figure 5. Insolation on Earth

takes into account the precise angle made by all surface elements on the star with the point on the planet under consideration and hence gives precise, non-zero instellation values. The contour plot-1 in Fig. 7 shows the ratio of instellation values predicted by this model over the values predicted by the IS law at the poles. We see higher values of the ratio at the upper-left extreme of the plot since the IS law heavily underestimates the instellation at the poles.

Another interesting aspect of this model is the distribution of instellation on the planetary hemisphere not facing the star. Unlike the IS model, the instellation here extends towards the night-side of the exoplanet thus shifting the day-night terminator. Contour plot-2 shows the maximum latitude up to which instellation is non-zero or the terminator angle from the equator. If we consider the latitude to go beyond its maximum value of 90 degrees along the sub-stellar longitude, then we see that for some exoplanets the instellation becomes zero at nearly 110-degree latitude or 20 degrees from the pole to the night-side of the exoplanet. For far-off planets, the terminator angle remains 90 degrees, and this is indicative of the fact that the IS law suffices for such exoplanets.

This model makes the theoretical basis for estimating the amount of irradiation in the proximity of the stellar surface. The results of this model can be easily tested for the Sun. The Parker solar probe which is bound to reach its perihelion at nearly 0.04 AU from the Sun in December 2025 would be useful to obtain observational data at a close distance to the Sun. The Poynting flux measured by the FIELDS instrument on the solar probe would be useful, as an observational benchmark, to verify the results. It has been earlier proposed that even small changes in stellar irradiance may cause fundamental climatic changes on an Earth-sized planet, which in turn could affect its habitability Kilic et al. (2017), Forget & Leconte (2014). The extent of difference in irradiation from the standard approach at the poles and the substellar point seems significant enough and is therefore likely to introduce appreciable changes in the current climate models of close-in Earth-size exoplanets.

This model derives the limb darkening coefficients using the data provided by Claret (2000). However, there have been more recent studies in this area, for instance, Claret & Bloemen (2011) that have not calculated bolometric coefficients since observations are wavelength specific. The model can be improved if the revised bolometric limb darkening coefficients from these recent studies can be obtained.

To better understand the behaviour of these patterns, we need an analytical estimation of instellation as a function of the stellar radius, semi-major axis, limb darkening coefficients and latitude. This would be useful to understand the most extreme cases that might exist but have not been observed. The python code *InstellCa* for calculating instellation patterns on exoplanets is made available to the community for further studies and can be accessed here.

ACKNOWLEDGEMENTS

I would like to thank Dr Martin Turbet for his suggestions and opinions regarding this work.

DATA AVAILABILITY

No new data were generated or analysed in support of this research.

REFERENCES

Budaj J., 2011, The Astronomical Journal, 141, 59
Chen K.-Y., Rhein W. J., 1969, Publications of the Astronomical Society of the Pacific, pp 387–398
Claret A., 2000, Astronomy and Astrophysics, 363, 1081
Claret A., Bloemen S., 2011, Astronomy & Astrophysics, 529, A75
Forget F., Leconte J., 2014, Philosophical Transactions of the Royal Society A: Mathematical, Physical and Engineering Sciences, 372, 20130084
Fröhlich C., 2000, Space Science Reviews, 94, 15
Horvat M., Conroy K. E., Jones D., Prša A., 2019, The Astrophysical Journal Supplement Series, 240, 36
Kilic C., Raible C., Stocker T., 2017, The Astrophysical Journal, 844, 147
McCluney W. R., 2014, Introduction to radiometry and photometry. Artech House
Stevenson K. B., et al., 2014, Science, 346, 838
Wilson R., 1990, The Astrophysical Journal, 356, 613
Wood D. B., 1973, Monthly Notices of the Royal Astronomical Society, 164, 53

This paper has been typeset from a TEX/LATEX file prepared by the author.

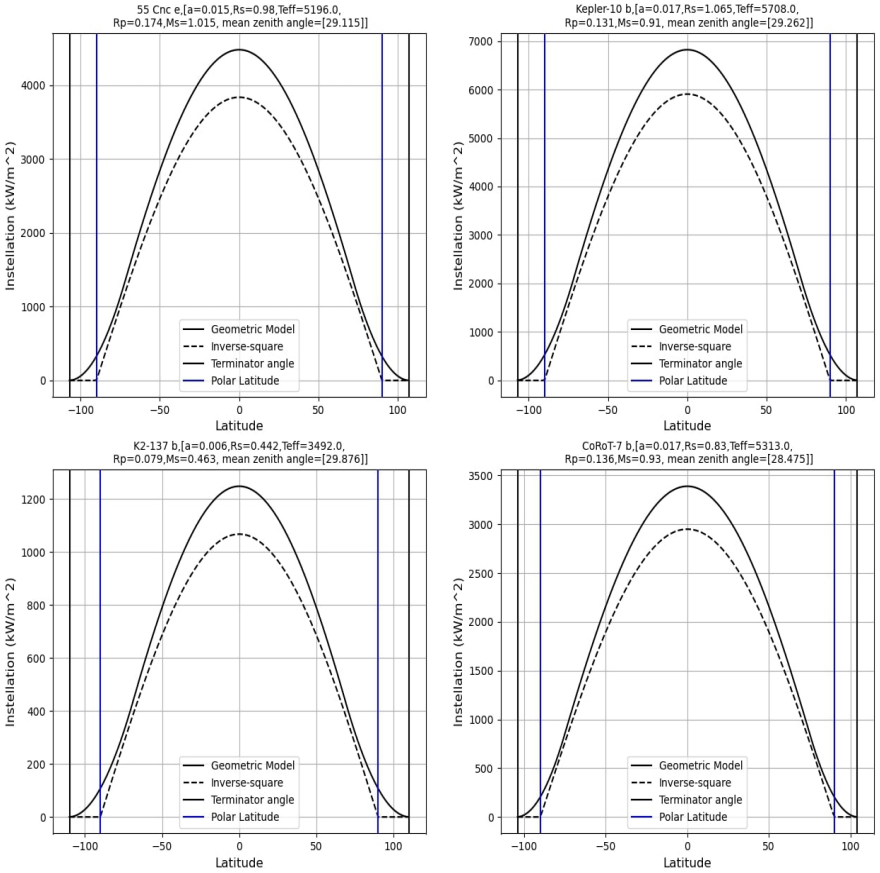

Figure 6. Instellation pattern for close-in planets Kepler-10 b, 55 Cnc e, CoRoT-7 b and K2-137 b

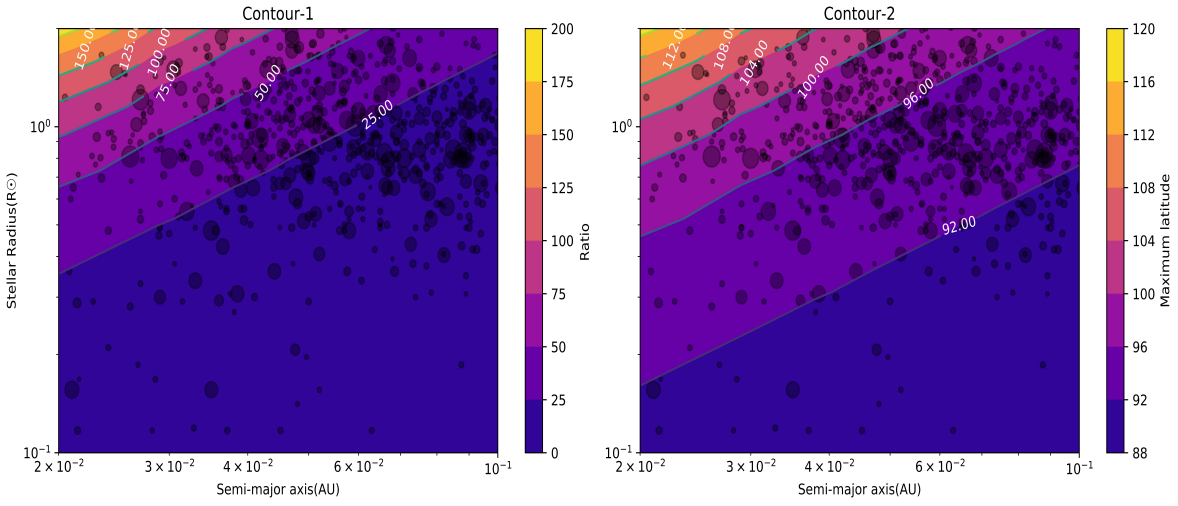

Figure 7. Contour plot-1 depicts the ratio of instellation at the poles for the two approaches. Contour plot-2 depicts the angle of the terminator from the equator. The black spots represent the parameters for the current exoplanet population with spot size proportional to the planetary size.